Unravelling the molecular mechanisms underlying mitochondrial dysfunction in metabolic diseases

Mposhi, Archibold

DOI:
10.33612/diss.146092791

CHAPTER THREE

A role of mitochondrial DNA methylation in mitochondrial dysfunction in NAFLD

Archibold Mposhi[1,2], Janette Heegsma[2], Vincent E. de Meijer[3], Bart (A.J.A.) van de Sluis[4], Svenja Sydor[5], Lars P. Bechmann[5], Ikbal Agah Ince[1], Klaas Nico Faber[2] and Marianne G. Rots[1].

[1]Department Pathology and Medical Biology, University of Groningen, University Medical Center Groningen, Groningen, The Netherlands

[2]Department of Gastroenterology and Hepatology, University of Groningen, University Medical Center Groningen, Groningen, The Netherlands.

[3]Department of Surgery, Division of Hepato-Pancreato-Biliary Surgery and Liver Transplantation, University Medical Center Groningen, University of Groningen, Groningen, the Netherlands

[4]Section of Molecular Genetics, University Medical Center Groningen, University of Groningen, Groningen, the Netherlands

[5]Department of Internal Medicine, University Hospital Knappschaftskrankenhaus, Ruhr-University Bochum, Bochum, Germany

Manuscript in preparation

ABSTRACT

Hepatic lipid accumulation and mitochondrial dysfunction are hallmarks of non-alcoholic fatty liver disease (NAFLD), yet molecular parameters underlying this disease and its progression are not well understood. Differential methylation within the mitochondrial DNA (mtDNA) has been suggested to be associated with dysfunctional mitochondria and with NAFLD progression. This study further investigates whether mtDNA methylation is associated with NAFLD and whether it is a cause or consequence of increased lipid accumulation.

The effects of mtDNA methylation on mitochondrial function were investigated by constructing HepG2 cells to stably express mitochondria-targeted prokaryotic cytosine DNA methyltransferases (M.CviPI/M.SssI for GpC/CpG methylation, respectively). A catalytically-inactive variant (M.CviPI†) was included as a control. Mitochondrial gene expression and metabolic activity were impaired while lipid accumulation was increased in HepG2-mtMCviPI and HepG2-mtMSssI cells compared to the controls. To test whether lipid accumulation causes mtDNA methylation, wildtype HepG2 cells were subjected to fatty acid treatment for 2 weeks. Although the expression of mitochondrial genes was reduced (except for *ND6*), no clear differences in mtDNA methylation were observed. To assess the effects of *in vivo* parameters, livers from mice fed a high-fat high cholesterol diet (HFC for 6 or 20 weeks) and from patients with NAFLD were analyzed for mtDNA methylation and gene expression. Hepatic *ND6* mitochondrial gene expression and cytosine methylation in the *ND6* region were increased in both HFC mice and patients with NAFLD when compared to controls, while mtDNA copy number was unchanged. This study supports a role for mtDNA methylation in promoting mitochondrial dysfunction and impaired lipid metabolism. However, differential mtDNA methylation does not seem to be a direct consequence of lipid accumulation. Other *in vivo* factors such as inflammation and/or fibrosis need to be investigated for their role in promoting mtDNA methylation.

INTRODUCTION

Mitochondria, as the main cellular energy producers, are the key drivers of metabolism and mitochondrial dysfunction results in variety of (metabolic) diseases, including non-alcoholic fatty liver disease (NAFLD)[1,2]. Mitochondria contain their own circular genome (mtDNA), which is approximately 16 kb in size and encompasses 37 genes: 13 protein-coding genes, 2 ribosomal RNAs (rRNAs), 22 transfer RNAs (tRNAs)[3-5] and some other non-coding RNAs with unknown function[6].

NAFLD is an umbrella term for a spectrum of pathologies associated with fat accumulation in the liver, including simple steatosis, non-alcoholic steatohepatitis (NASH), NASH-associated fibrosis and cirrhosis, which predisposes for hepatocellular cancer (HCC). During the progression of NAFLD, mitochondria undergo structural and molecular changes that impair their function[7]. The mitochondrial genome itself plays a role in the development and progression of NAFLD. For instance, individuals with mitochondrial haplogroup H share a common single nucleotide polymorphism (SNP) in the mtDNA and are more susceptible to NASH, while those with haplogroup L appear relatively protected against NASH and fibrosis[8]. Furthermore, during the transition from simple steatosis to NASH, hepatic mitochondrial plasticity is lost and this impairs the ability of the liver to adapt to oxidative stress[9]. Surprisingly, NASH patients have a higher mitochondrial content (measured as mitochondrial copy number), but a lower mitochondrial maximal respiration[9,10] compared to lean controls without NAFLD. Thus, it appears that there is an extra layer of mtDNA regulation that causes mitochondrial dysfunction by decreasing the respiratory capacity in NASH patients.

The regulation of mtDNA replication and transcription has been extensively studied[5,11-15], but intricate details on how mitochondrial gene expression is regulated remain elusive. The mtDNA contains a non-coding regulatory region, known as the displacement loop (D-loop), which houses three promoter regions, namely, HSP1 and HSP2 for the outer Heavy-strand and LSP for the inner Light-strand[12,16]. These promoters are responsible for the transcription of multiple genes in polycistronic transcripts: The HSP1 regulates transcription of *12S* and *16S* ribosomal RNAs, while the HSP2 promotes transcription of the entire H-strand as a polycistronic transcript containing twelve of the thirteen protein-coding genes. The LSP on the other hand

regulates the transcription of just one protein-coding gene, e.g, the complex 1-subunit *ND6*, and eight tRNAs.

It has been suggested that epigenetic modifications, such as 5-methylcytosine (5mC), on the mtDNA play a role in regulating the expression of mitochondrial genes[17-22] and as such might provide a novel class of biomarkers for metabolic diseases. MtDNA methylation is negatively associated with mtDNA transcription[23]. Methylation of mtDNA could serve as an adaptation to cellular stress that enables the mitochondria to function in various harsh conditions. For instance, in the yeast *Candida albicans,* continuous exposure to hypoxic conditions decrease mtDNA methylation[24]. Importantly, this phenomena has also been observed for mammalian mtDNA in response to external stress factors, such as air pollution[25-28],and exposure to arsenic-contaminated water [29].

Numerous studies have shown that differential mtDNA methylation associates with clinical phenotypes in diseases such as diabetes, colon cancer, Alzheimer's disease, as well as in aging[7,21,22,30,31]. Interestingly, mtDNA has a peculiar non-CpG methylation pattern, which reflects its prokaryotic origin[4,32,33]. Importantly, DNA methyltransferases (DNMTs)[34-36] have indeed been reported to be present in the mitochondria. Modulating the expression of these DNMTs by overexpression or gene-knock down resulted in increased and decreased mtDNA methylation, respectively[20,33]. Despite these intriguing indications that mtDNA methylation plays a biological role in cell physiology, the actual existence of mtDNA methylation is still heavily debated. This debate is in part fueled by the technical challenges involved in determining methylation in the tightly coiled mtDNA structures. For instance, techniques such as pyrosequencing depend on bisulfite conversion and are prone to bias if cytosine residues are resistant to conversion. The supercoiled structure of mtDNA promotes bisulfite resistance by preventing the complete conversion of unmethylated cytosines, which results in an overestimation of methylation[37-40]. The supercoiled structure can be relaxed by fragmenting the mtDNA with restriction endonucleases or sonication, thereby improving bisulfite conversion efficiency[37-39]. Importantly, however, differential mtDNA methylation is also detected when using bisulfite-independent techniques, such as methylated DNA immunoprecipitation (MeDIP)[41] and mass spectrometry[20,42].

For NALFD, the relationship with mitochondrial dysfunction has been extensively described, although the exact mechanisms initiating steatosis and its subsequent

progression to NASH remain elusive. It is known that the development of NAFLD depends on a myriad of factors that include obesity, insulin resistance, as well as genetic predisposition. Interestingly, whether epigenetic changes in mtDNA can initiate mitochondrial dysfunction in the liver remains to be established. Using methylation-specific PCR on intact mtDNA, Pirolla et al.[7] provided the first indication that NASH patients show hyper-methylated mtDNA in the *ND6* region compared to patients with simple steatosis. Although the difference is small, the higher methylated/unmethylated mtDNA ratio in NASH samples associated with a decreased *ND6* gene and protein expression compared to simple steatosis[7].

Here, we first set out to address the functional effects of mtDNA methylation in liver cells. We artificially expressed mitochondrial-targeted DNA methyltransferases in HepG2 cells to assess the effect on cellular lipid accumulation and mitochondrial function. Complementary, we assessed the effect of lipid exposure of HepG2, as well diet-induced NAFLD in mice and patients, on mtDNA methylation. Our findings support a role of mtDNA methylation in the development and progression of NAFLD.

MATERIAL AND METHODS

Cell and culture conditions

Human hepatocarcinoma cells (HepG2) (ATCC, Manas, VA, USA) were cultured in Dulbecco's Modified Eagle Medium (DMEM) + GlutaMAX (Gibco, Carlsbad, CA, USA) supplemented with 1% Penicillin-Streptomycin-Fungizone (PSF) and 10% Fetal Calf Serum (FCS) (Lonza, Verviers, Belgium) at 37°C in a humidified 5% CO_2 incubator. Human embryonic kidney cells, Hek293T (ATCC) were cultured in DMEM + GlutaMAX (Gibco) with similar supplementation to HepG2 cells. During transfection, DMEM was supplemented with 1% PSF and 5% FCS (Lonza) at 37°C in a humidified 5% CO_2 incubator.

Plasmids and Constructs

Previously, mitochondria targeted MCviPI, MCviPI† (catalytically inactive) and MSssI were cloned in pCDH-CMV-MCS-SV40-puro plasmid[19]. The resultant pCDH-CMV-master synthetic construct-conII-SV40-puro containing a mitochondrial localization signal, (MLS) – HA-tag-flexible linker- [MSssI/ MCviPI/ MCviPI†] and two NES (nuclear export signal) were subsequently used for transductions. Hek293T cells were seeded at 700,000 cells per well in a 6-wells plate for 16 hours. After cells had reached 70 – 80% confluency, polyethylenimine (PEI) (Sigma-Aldrich, St. Louis, USA) and plasmid DNA (pCDH-MSssI/ MCviPI/ MCviPI†) were added at a volume to mass ratio of 1:4 (**Supplementary Table S1**). After 48 hours, medium containing virus particles was collected and filtered directly onto HepG2 cells using a 0.45µmol/L millex HV PVDF filter (Merck Millipore, Darmstadt, Germany). To validate expression of the methyltransferase, qPCR was performed using primers that recognize the target sequences (**Supplementary Figure S1B-C**). Antibiotic selection was carried out on HepG2-MCviPI, HepG2-MCviPI†, and HepG2-MSssI using different concentrations of puromycin (1 – 4 µg/ml) (**Supplementary Figure S1C**).

Animals

C57BL/6J mice (Charles River, Saint-Germain-Nuelles, France) were age- and sex-matched (8-10 weeks old). Mice were then fed either regular chow or high fat, high cholesterol (HFC) diet containing 21% fat, with 45% calories from butter-fat and 0.2% cholesterol per gram of diet (Scientific Animal Food and Engineering (SAFE),

Villemoisson-Sur-Orge, France) for 6 weeks (n=6; 6wkHFC) or 20 weeks (n=8; 20wkHFC) similar to earlier studies[43,44]. Animals were kept in a pathogen-free environment with alternating dark-light cycles of 12 hours, controlled temperature (20-24 ºC) and relative humidity (55%±15%). 6wkHFC animals were housed in the animal facility of the Otto-von-Guericke University hospital Magdeburg according to the recommendations of the Federation of European Laboratory animals (FELASA). All procedures were approved by the Landesamt für Natur-, Umwelt-, und Verbraucherschutz Northrhine Westfalia (LANUV NRW) and the Landesverwaltungsamt Saxony-Anhalt (reference number: 84.0204.2013.A082). 20wkHFC animals were housed under standard laboratory conditions according to the Dutch law on the welfare of laboratory animals and guidelines of the ethics committee of University of Groningen for care and use of laboratory animals. Animals received food and water *ad libitum* and were fasted 4 hours before termination. Tissues were snap-frozen in liquid nitrogen or fixed in paraformaldehyde.

Human liver samples

Investigations in human material and the use of patient liver samples were approved by the Ethics Committee (Institutional Review Board) of the University Hospital Essen (Reference Number: 09-4252) and the study protocol conformed to the ethical guidelines of the Declaration of Helsinki. Sample allocation for patients that underwent bariatric surgery was undertaken following patients' informed consent. Liver samples from eight patients and five healthy control individuals (without NAFLD) were collected during surgery.

Free fatty acid preparation

Sodium palmitate (PA)(Sigma-Aldrich) and/or Sodium oleate (OA)(Sigma-Aldrich) were dissolved in phosphate buffered saline (PBS)(Gibco) and placed in a water bath for 1 hour at 70ºC. 10% fatty acid free bovine serum albumin (BSA) (Sigma-Aldrich) was dissolved separately in PBS at 37ºC. 10 mmol/L stock solutions of PA/OA (molar ratio 1:2) and PA only were prepared by mixing the 10% BSA solution with the PA/OA solution at room temperature to allow for conjugation.

Oil Red O staining (ORO)

ORO (Sigma-Aldrich, O-0625) was dissolved in 99% 2-propanol on a roller mixer overnight at room temperature. The solution was filtered using Whatman size 4 filter paper (Whatman International, Buckinghamshire, UK) and diluted with demi-water at a ratio of 2 parts water and 3 parts ORO solution. Prior to staining, cells were fixed with 4% Formaldehyde for 10 minutes. Cells were then rinsed with 60% isopropanol for 30 seconds. ORO stain was applied to the cells for 10 minutes and removed. Cells were rinsed again with 60% isopropanol for 5 seconds. Cells were rinsed with demi-water for approximately 1 minute and Mayer's hematoxylin solution (Sigma) was added for 10 minutes. The cells were then rinsed twice for 30 seconds with demi-water, air-dried and mounted with Crystal/MountTM (Biomeda Corp, Foster City, CA, USA).

RNA isolation and Quantitative reverse transcriptase PCR (qRT-PCR)

Total RNA was extracted from HepG2 cell lines using Trizol (Sigma-Aldrich) and quantified using a Nanodrop 1000 spectrophotometer (Thermo Scientific, Waltham, MA, USA). 2.5 µg RNA was treated with DNaseI (Thermo Scientific) and reverse transcribed using random hexamer primers with M-MLV Reverse transcriptase to generate cDNA, according to the manufacturer's protocol (Thermo Scientific). Each qRT-PCR reaction contained 10 µmol/L of the antisense and sense primers (**Supplementary Table S2**) (Sigma-Aldrich), 10 ng cDNA, and 2x ABsolute QPCR SYBR Green Rox Mix (Thermo Scientific). Real-Time qPCR was carried out on the ViiA7 Real-time PCR system (Applied Biosystems, Thermo Fisher Scientific, Waltham, MA, USA) for 15 min at 95ºC, followed by 40 cycles of 15 sec at 95ºC, 30 sec at 60ºC and 30 sec at 72ºC. *β-actin* was used as the house-keeping gene for nuclear and mitochondrial genes. Relative expression compared to controls was calculated using the ΔΔCt method[45].

Total DNA isolation, mitochondrial DNA isolation and mitochondrial copy number determination

HepG2 cells were harvested and cell pellets were snap-frozen in liquid nitrogen for storage. Cell lysis was performed overnight at 55ºC in TNE lysis buffer (10 mmol/L Tris/HCl, pH 7.5; 150 mmol/L NaCl; 10 mmol/L EDTA; 1% SDS) and 100 µg

Proteinase K. Total cellular DNA, including nuclear and mitochondrial DNA, was extracted using chloroform/isoamyl alcohol (24:1), treated with RNase A (Thermo Scientific) for 1 hour at 37ºC, and then precipitated using isopropanol. DNA concentrations were quantified using a Nanodrop 1000 spectrophotometer (Thermo Scientific, USA). Human and mouse mtDNA copy number was determined by qPCR using primers designed for CYTB versus β-actin and COX2 versus RSP18, respectively[46] (**Supplementary Table S2**).

Frozen human and mouse liver samples were homogenized using a pestle tissue grinder. Total DNA and RNA were extracted using the AllPrep DNA/RNA/Protein Mini Kit (Qiagen, Hilden, Germany) according to the manufacturer's protocol. Mitochondrial DNA was isolated with the Mitochondrial DNA isolation kit (Abcam, Cambridge, UK), according to the manufacturer's instructions. The DNA and RNA concentrations in each sample were measured by the NanoDrop 1000 spectrophotometer (Thermo Scientific).

Pyrosequencing and sample preparation

One µg of DNA was first linearized using *Bam*HI (*fast digest*, Thermo Scientific) at 37ºC for 1 hour. 500 ng of DNA was then bisulfite-converted using the EZ DNA methylation Gold Kit (Zymo Research, Irvine, CA, USA) according to the manufacturer's instructions. For pyrosequencing, bisulfite PCR of the *CSBII/III*, *COX1, D-loop*, *HSP1*, *LSP,* and *ND6* regions was conducted using bisulfite-specific primers (**Supplementary Table S3**) at specific annealing temperatures (Note: *HSP2* region was not analyzed due to low quality of pyrosequencing primers). Primers were designed using the PyroMark Assay Design 2.0 software (Qiagen) and a BLAST search (https://blast.ncbi.nlm.nih.gov/Blast) was carried out to identify nuclear mitochondrial DNA sequences (NUMTs). The PCR product was then run on a 2% agarose gel to confirm amplification and predicted amplicon length. The PCR product was then sequenced using the Q48 automated pyrosequencing machine (Qiagen) according to the manufacturer's instructions. The percentage methylation at each CpN site was determined using the PyroMark Q48 Autoprep 2.4.2 software (Qiagen).

Methylation-Specific PCR (MSP)

Bisulfite-converted DNA was used as the template for a methylation-specific polymerase chain reaction (MS-PCR). Two previously reported[7] pairs of primers were used, that is, one pair specific for bisulfite-converted methylated DNA (M primers) (Sigma-Aldrich) and the other pair specific for bisulfite-converted unmethylated DNA (U primers). Each qPCR reaction contained 10 µmol/L of the antisense and sense primers (M/U primers)[7] (**Supplementary Table S4**), 5 ng DNA and 2x ABsolute QPCR SYBR Green Rox Mix (Thermo Scientific). PCR was carried out on the ViiA7 Real-time PCR system (Applied Biosystems, Thermo Fisher Scientific) for 15 min at 95^{O}C, followed by 40 cycles of 15 sec at 95^{O}C, 30 sec at 60^{O}C and 30 sec at 72^{O}C. Results were presented as ratios of CT values obtained for M primers vs U primers normalized against CT values for U primers targeting the D-loop. The resulting ratios were expressed as methylated DNA vs unmethylated DNA, as reported previously[7].

Oxygen consumption rate (Seahorse)

Mitochondrial oxygen consumption rate (OCR) was measured using the Seahorse XFe24 analyzer (Seahorse Bioscience, Inc., Billerica, MA, USA). HepG2 cells were seeded at 7.5 x 10^5 cells/ well in 24-well Seahorse utility plate 24 hours prior to OCR measurement. OCR was then measured according to the manufacturer's instructions. Raw data was normalized to protein content and all analysis was conducted using Wave 2.6.0.31 software (Agilent Technologies, Santa Clara, CA, USA).

Microscopy

To visualize mitochondria, an antibody against the mitochondrial protein MnSOD (manganese superoxide dismutase) was used. HepG2 wild type cells and transgenic derivatives were cultured on glass coverslips for 24 hours. At the termination of the experiment, cells were washed with ice-cold PBS and fixed with 4% paraformaldehyde (PFA) (Merck Millipore, Darmstadt, Germany) for 10 min. Cells were permeabilized using 0.1% Triton-X100 for 10 min at room temperature. Blocking was performed with 2% BSA for 30 min and cells were incubated with an anti-MnSOD2 antibody (Enzo Life Sciences, Brussels, Belgium) at a dilution of 1:1,000 for 1 hour. Cells were washed and incubated with the secondary antibody, goat-anti-rabbit Alexa-488 (Invitrogen by Thermo Scientific, Waltham, USA). Coverslips were mounted onto glass slides using

Vectashield mounting medium with DAPI (Vector Laboratories, Inc., Peterborough, UK) and fluorescence was visualized using a Leica DMI6000B inverted microscope (DFC365 FX camera) (Leica Microsystems, Wetzlar, Germany).

Database analysis

NAFLD-related RNAseq data from the Sequence Read Archive (SRA) database were searched using the following keywords: "Human, Liver, Nonalcoholic Fatty Liver Disease, RNA" resulting in ninety-one data set search hits from three different projects. Fifty-seven of which belong to the BioProject PRJNA523510 transcriptome dataset on various stages of NAFLD, downloaded from NCBI's SRA database (http://www.ncbi.nlm.nih.gov/sra) under the accession number SRP186450 (https://trace.ncbi.nlm.nih.gov/Traces/sra/?study=SRP186450). Overview of differentially expressed mitochondrially-encoded hepatic gene profiles between healthy normal weight controls and NAFLD patients[47] were analyzed using the DESeq2 software (Geneious Biologics, Auckland, New Zealand) (https://www.geneious.com/tutorials/expression-analysis-deseq2).

Statistics

Data are expressed as the means ± SEM of at least 3 independent experiments performed on cell line panels created at three independent time points. Statistical analysis was performed using Graph-pad Prism 7 software. Single group comparisons were performed with the two-tailed unpaired student's t-test. Human and mouse data were analyzed using a two-tailed Mann Whitney U test. Correlation analysis was conducted using Spearman's correlation test and P values ≤0.05 were considered significant. In this study, our comparative analysis approach was hypothesis driven. Therefore, to present the reader with all the results, we did not adjust our significance levels for multiple testing, as previously suggested[48]. A p-value < 0.05 was considered statistically significant (*p≤0.05, **p<0.01 and ***p<0.001).

RESULTS

Enhanced methylation of mtDNA in HepG2 transgenic cell lines expressing mitochondria-targeted mCviPI or MSssI

A general overview of the distribution of cytosine residues in the human mtDNA shows that 8.3% of cytosines are in the CpG context, while 13.5% are in the GpC context (**Figure 1A**). 4.0% of all cytosines occur in both CpG and GpC contexts (GpCpG). Pyrosequencing of DNA (at various regions, **Figure 1B**) derived from mitochondria-targeted MCviPI- or MSssI-expressing HepG2 cells revealed that the mitochondria-targeted prokaryotic methyltransferases induced methylation of mtDNA in the expected GpC and CpG context, respectively (**Figure 1C-F**). In this study, 35.3% of the cytosines analyzed were in the CpG context while 47.1% were in the GpC context. The induced methylation across the targeted cytosines ranged from 5.2% to 40.0% and 10.7% to 42.3% for MCviPI and MSssI, respectively. The cytosine at GpC/CpG position 526 is targeted by both enzymes and resulted in 19.4 ± 1.3% methylation for M.CviPI versus 28.7 ± 1.0% for M.SssI Figure 1F), while the GpC/CpG at position 163 showed 38.5 ± 1.5% methylation for M.CviPI versus 24.0 ± 3.6% for M.SssI (**Figure 1C)**. Interestingly, the cytosine at position 329 (GpC) within the conserved sequence block 3 (CSBIII) was resistant to MCviPI-induced methylation (**Figure 1D**), while the cytosine at position 389 (TCT) was methylated by M.SssI (**Figure 1E**).

Baseline methylation readings were obtained for all cytosines, also in the wildtype cells (depending on the position ranging from about 2% – 15% unconverted cytosines), which did not further decrease after digesting the mtDNA at three positions using *Hind*III, as compared to a single cut with *Bam*HI (**Supplementary Figure S2A, B**). For instance, CpG position 545, which is 16 bp away from the HSP1 transcription start site had a high percentage of both induced (33.0 ± 3.5 for HepG2-mtMSssI) as well as control methylation (15.1 ± 4.3% for HepG2-mtMCviPI and controls: 14.9 ± 3.3% (HepG2-wt), 14.4 ± 2.8% (HepG2-mtMCviPI†)) (**Figure 1F**).

Interestingly, after 2 months in culture, the levels of induced mtDNA methylation were decreased in the transgenic cell lines (**Supplementary Figure S3A**), suggesting an endogenous silencing of the integrated prokaryotic methyltransferase expression cassette and/or a growth disadvantage due to mtDNA methylation. MtDNA methylation in HepG2-mtMCviPI was reduced (2.2%) to levels similar to the HepG2-WT and HepG2-mtMCviPI† controls (2.2 – 2.8%), while methylation in HepG2-mtMSssI also

decreased, albeit less pronounced (7.8%). To validate that the methyltransferases were selectively targeted to the mitochondria and not the nucleus[19], pyrosequencing was also conducted on a randomly selected nuclear promoter region (*UCHL1*, **Supplementary Figure S3B**). Results confirm that the methyltransferases mainly localized in the mitochondria since enhanced methylation of nuclear DNA was not detected for this reporter region.

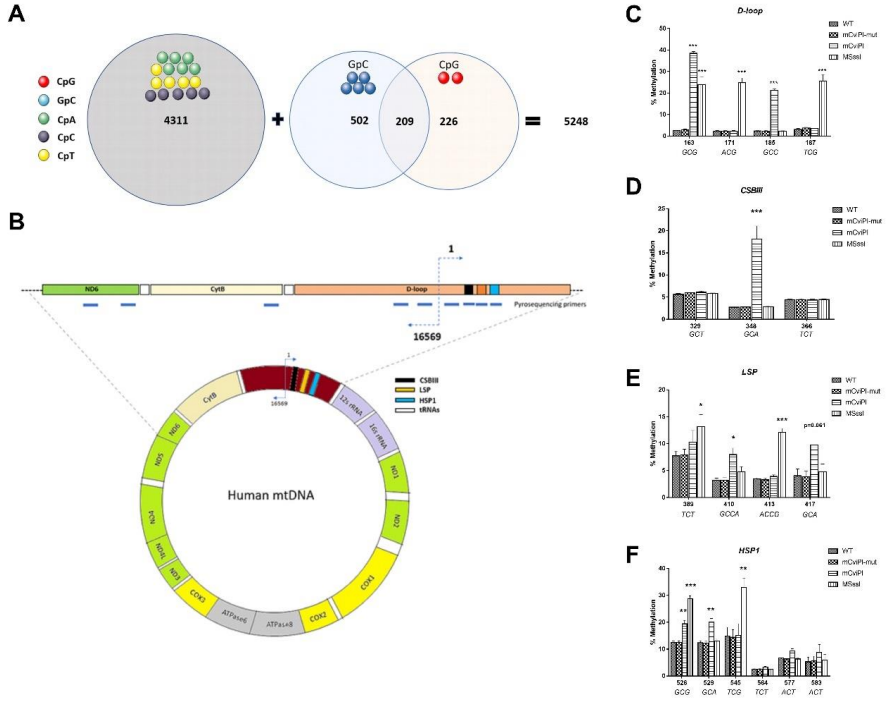

Figure 1: Methylation patterns in HepG2 cells expressing mitochondria-targeted methyltransferases (mCviPI or MSssI). A) Diagram representing the CpG/GpC distribution of cytosine residues in mtDNA; **B)** annotated human mitochondrial DNA showing regions analyzed in this study; **C)** a region in the *D-loop* (160 – 190*), OriH* (nucleotide 191); **D)** *CSBIII* (320 – 370); **E)** *LSP* (380 – 430) and; **F)** *HSP* (525 – 585) regions ±20bps; CpN positions: 163 = **GCG**, 171 = A**CG**, 185 = **GC**C and 187 = T**CG,** 329 = **GC**T, 348 = **GC**A, 366 = T**C**T, 389 = **TCT**, 410 = **GCC**A, 413 = A**CCG**, 417 = **GC**A**,** 526 = **GCG**, 529 = **GC**A, 545 = T**CG**, 564* = T**CT,** 577 = A**C**T and 583 = A**C**A. Each data point represents the mean ± SEM of three independently constructed transgenic cell and p values as *p≤0.05, **p<0.01 and ***p<0.001 with respect to the MCviPI mutant control.

CpG or GpC methylation of mtDNA downregulates the expression of mitochondrial genes in HepG2 cells

Previously, we have shown that artificially-induced GpC methylation of the mtDNA represses mitochondrial gene expression depending on the cell type[19]. To determine the effects of mtDNA methylation on mitochondrial gene expression in HepG2 cells, qRT-PCR was carried out on HepG2-mtMCviPI, its mutant control and HepG2-mtMSssI-expressing cells, as well as the HepG2 wild type control cells. No significant differences in mitochondrial gene expression were observed between wildtype HepG2 and HepG2-mtMCviPI† mutant controls for *HSP1* (*12S, 16S*)-, *HSP2* (*ND1, COX1, CYTB*)-, and *LSP* (*ND6*)-controlled genes (**Fig 2A-C**). In HepG2-mtMCviPI cells, the *12S* and *16S* RNA genes were significantly downregulated compared to HepG2-mtMCviPI† (66.6 ± 5.8% $p<0.01$ and 71.0 ± 9.1%, $p<0.05$ compared to expression in mutant cells set at 100%, respectively) (**Figure 2A**). No clear difference in gene expression was obtained due to the induced GpC methylation of the other genes tested. Interestingly, expression of all analyzed mitochondrial genes (*12S* and *16S , ND1, COX1, CYTB and ND6*) was decreased more than 50% in HepG2-mtMSssI, when compared to the mutant and parent control cells (**Figure 2A-C)**. The lower gene expression could not be explained by an effect in mtDNA copy number, as these numbers were not significantly different between the analyzed cell lines (**Figure 2D**). Actually, an even more pronounced lowering in expression was observed when gene expression was normalized to copy number (**Supplementary Figure S4**). These data show that induced methylation in the GpC context, and even more obvious for the CpG context, decreased mitochondrial gene expression, without lowering the mtDNA copy number in HepG2 cells.

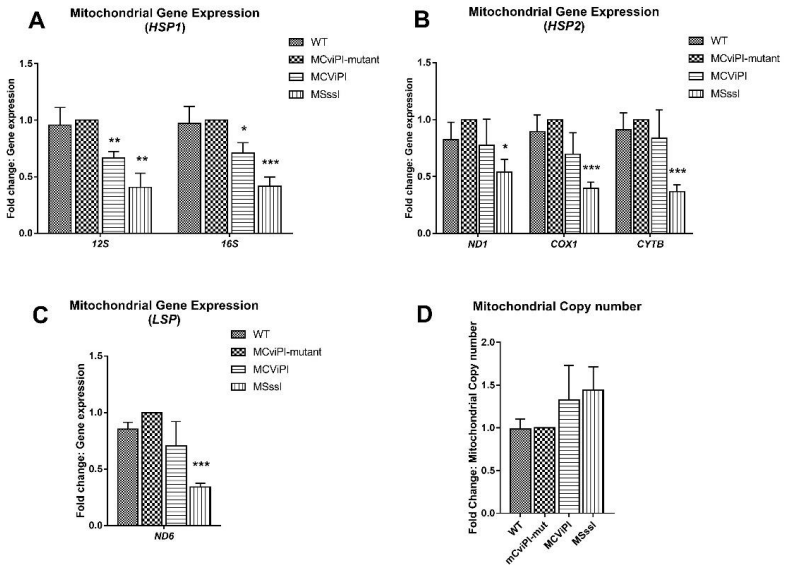

Figure 2: Normalized mitochondrial gene expression and mtDNA copy number in transgenic HepG2 lines expressing mitochondria targeted methyltransferases (mCviPI or MSssI). Expression of A) *HSP1*; B*) HSP2* and; C) *LSP* genes normalized against HepG2-mtMCviPI mutant control. D) Mitochondrial copy number in HepG2-mtMCviPI and -MSssI normalized against mutant control. Each data point represents the mean ± SEM of three independently constructed clones per transgenic cell line. Significance is demonstrated as *p≤0.05, **p<0.01 and ***p<0.001 with respect to the MCviPI mutant control.

MtDNA methylation impairs mitochondrial oxygen consumption rate and lipid metabolism

To investigate the effects of mtDNA methylation on mitochondrial function, the oxygen consumption rate (OCR) was measured for the various transgenic cell lines. HepG2-mtMCviPI showed a lower spare respiratory capacity (45.1%, $p<0.05$) and a trend towards lower basal metabolic rate ($p = 0.082$) compared to the HepG2-mtMCviPI† control (**Figure 3)**. Other parameters measured, such as coupling efficiency and non-mitochondrial respiration, were not significantly affected compared to the control. Also, for MSssI (performed for two independently created cell lines panels), a similar pattern showing impaired mitochondrial function was observed (**Supplementary Figure S5**). As the mitochondrial structure is closely associated with the energetic state and function of mitochondria, mitochondria were stained to visualize their structure and

distribution in the transgenic HepG2 cells. No overt differences were observed between the transgenic lines and their respective controls (**Supplementary Figure S6**).

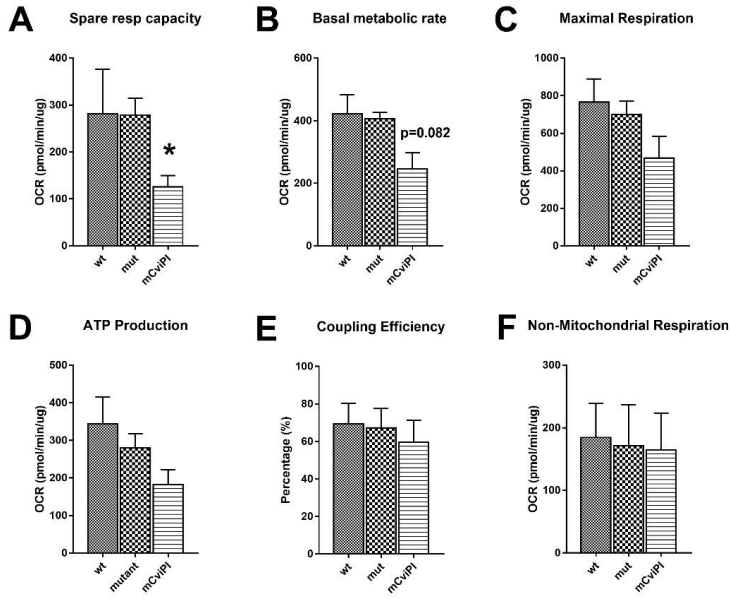

Figure 3: Mitochondrial Oxygen consumption rate in HepG2 cells expressing mitochondria targeted mCviPI. A-F) Mitochondrial respiration was determined in HepG2- WT, HepG2-mCviPI-mutant and HepG2-MCviPI. Each data point represents the mean ± SEM of three independently constructed transgenic cell and p values as *p≤0.05, **p<0.01 and ***p<0.001 with respect to the MCviPI mutant control.

To assess whether an impaired lipid metabolism was related to mtDNA methylation status, we measured lipid accumulation in the transgenic cell lines. Interestingly, control-grown HepG2-mtMCviPI cells already showed a trend towards increased lipid accumulation as measured by Oil red O staining intensity (**Figure 4A, C** and quantification in **G**). After treatment with palmitic acid and oleic acid, both HepG2-mtMCviPI and HepG2-mtMSssI showed increased lipid accumulation (**Figure 4B, D, F** and quantification in **H**). Taken together, these data show that methylation of mtDNA impairs mitochondrial function and promotes lipid accumulation in HepG2 cells.

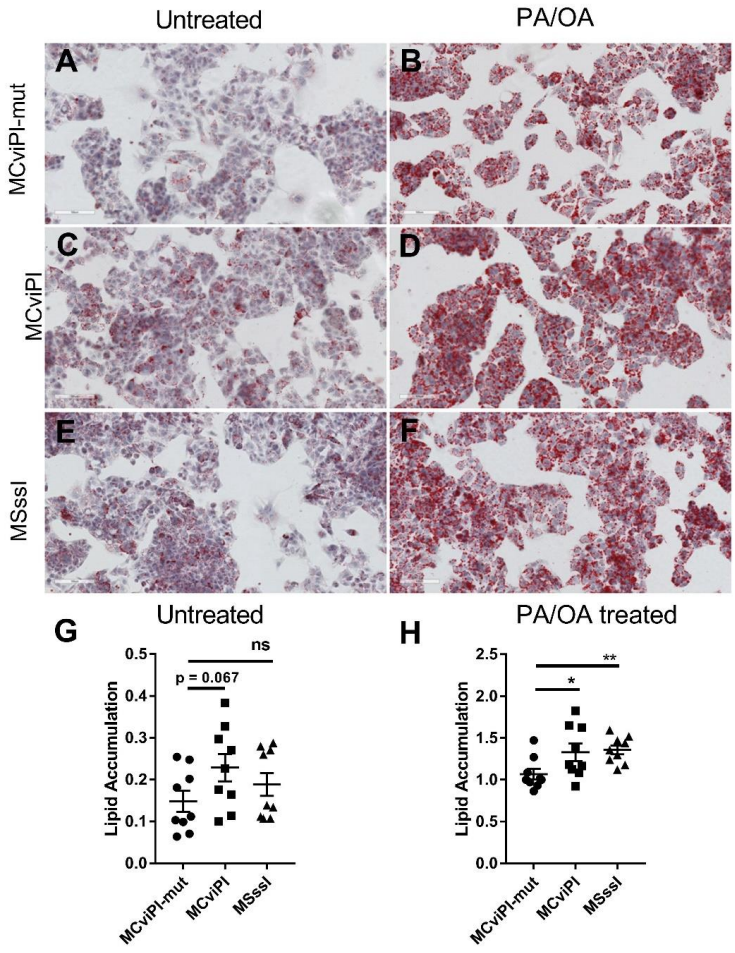

Figure 4: Oil Red O staining in HepG2 cells expressing mitochondria targeted methyltransferases (mCviPI or MSssI) after treatment with free fatty acids (PA/OA). Representative analysis and quantification of lipid accumulation in **A)** HepG2-MCviPI mutant; **B)** HepG2-MCviPI mutant treated with PA/OA (1mmol/l); **C)** HepG2-MCviPI; **D)** HepG2-MCviPI treated with PA/OA (1mmol/l); **E)** HepG2-MSssI; **F)** HepG2-MSssI treated with PA/OA (1mmol/l); **G)** Oil red O quantification for untreated cells (A, C, E); **H)** Oil red O quantification for PA/OA treated cells (B, D, F) using ImageJ software. Quantification data represent nine randomly taken pictures. *p≤0.05, **p<0.01 and ***p<0.001 with respect to the PA/OA treated MCviPI mutant control.

Exposure to palmitic acid affects mitochondrial and nuclear gene expression, but does not induce mtDNA methylation.

Monosaturated fatty acids are known to accumulate in hepatocytes during the progression of NASH[49,50] where they promote hepatic damage. In order to investigate whether mtDNA methylation can occur as a consequence of such lipid accumulation, HepG2 cells were exposed to palmitic acid (PA) for one or two weeks, or for two weeks followed by two weeks of recovery in normal medium without fatty acids (**Figure 5A**). Pyrosequencing resulted in highly reproducible patterns of mtDNA methylation in these HepG2 cell lines, ranging from 0.61% to 7.7% methylation at select GpC and CpG sites, but neither PA treatment schedule induced any differential mtDNA methylation (**Figure 5B, C, D**).

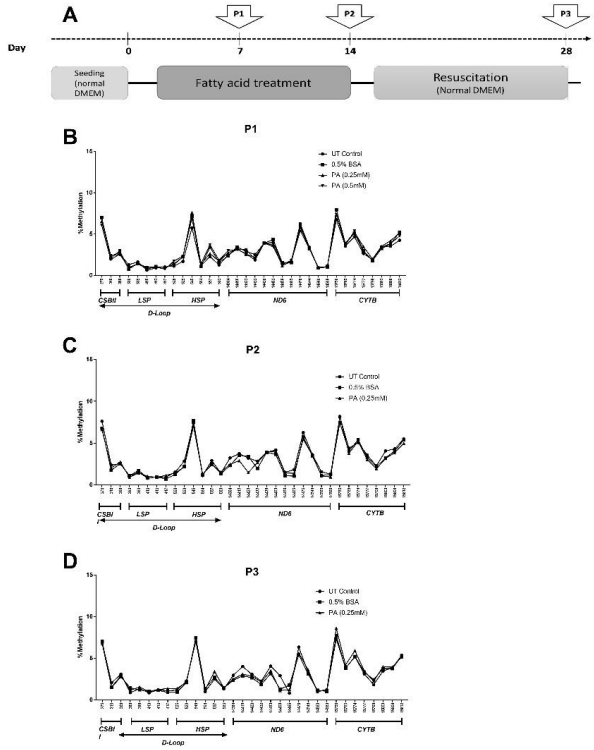

Figure 5: MtDNA methylation profile in HepG2 cells after long-term treatment with fatty acids (Palmitic acid). A) Treatment scheme with arrows indicating the day of sampling (**P1**: day 7; **P2**: day 14; **P3**: day 28); B – D) HepG2 cells treated with 0.25 – 0.5mmol/l palmitic acid (PA) for 1 or 2 weeks (P1, P2) and; D) HepG2 cells treated PA followed by an additional 2 weeks (P3) on resuscitation medium without PA (n=1).

Lowest methylation values were found for the *LSP* region (1.3%) compared to the *HSP* (2.7%), *ND6* (2.7%) and *CYTB* (4.1%) analyzed regions. The 1 or 2 week exposure of HepG2 cells to PA decreased mitochondrial gene expression (ranging from ~35% – 60%), but expression of all genes recovered after recovery of the cells in medium without PA (**Figure 6A**). Interestingly, *ND6* expression remained relatively unchanged during the prolonged PA exposure (P2) and returned to the normal expression levels when compared to the untreated HepG2 cells. In contrast, PA treatment induced the expression of nuclear genes involved in mitochondrial biogenesis (*PPARGC1A, NRF1,* and *TFAM*) (**Figure 6A**). This effect was most pronounced at week 2 (P2), but was not associated with an increase in mtDNA copy number.

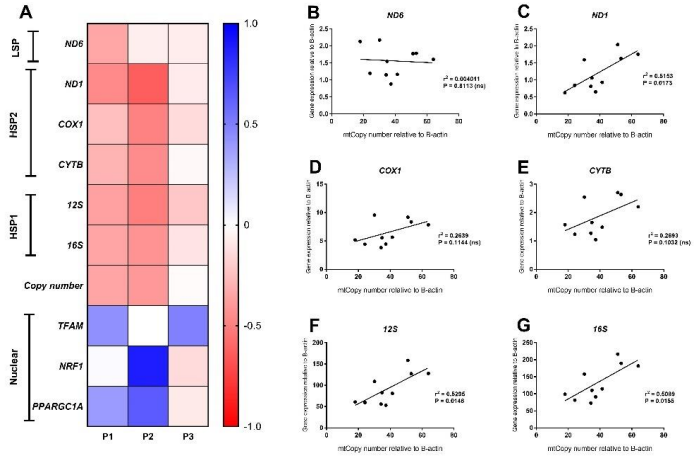

Figure 6: Mitochondrial and nuclear gene expression in **A**) HepG2 cells after treatment with 0.25mmol/l palmitic acid (PA) for 1 or 2 weeks (P1, P2) and then an additional 2 weeks on resuscitation medium without PA (P3); **B-G**) Correlation analysis of mitochondrial gene expression versus mtCopy number for HepG2 cells at P1 (treatment with 0.25mmol/l and 0.5mmol/l PA for 1 week, P2 (treatment with 0.25mmol/l PA) and P3 (additional 2 weeks on resuscitation medium without PA, **B**) *ND6*; **C**) *ND1*; **D**) *COX1*; **E**) *CYTB*; **F**) 12*S* and; **G**) *16S*.

Consistent with the generally accepted notion that mtDNA copy numbers correlate with gene expression, mitochondrial content positively correlated with *ND1*, *12S* and *16S* gene expression ($r = 0.72$, $p < 0.05$, $r = 0.73$, $p < 0.05$ and $r = 0.71$, $p < 0.05$, respectively). Intriguingly, no correlation was observed between *ND6*, *CYTB,* and *COX1* expression and mtDNA copy number (**Figure 6B-G**). These differences could be due to post-transcriptional mtRNA processing involving proteins like GRSF1,

FASTKD4, and TACO1**.** Expression of *GRSF1* (responsible for *ND6* mRNA processing) and *TACO1* (affecting *COX1*), was not consistently affected by PA treatment (**Figure 7A, B)**. Interestingly, *FASTKD4* which affects the bulk of mtRNAs, was downregulated by PA treatment to about 60% and this downregulation was sustained after reculturing the cells in normal (PA-free) medium. Overall, in this generally accepted *in vitro* model of lipid-mediated cell stress, we did not observe that excessive cellular lipid accumulation modulates mtDNA methylation, but the effect of lipids on mitochondrial gene expression was evident.

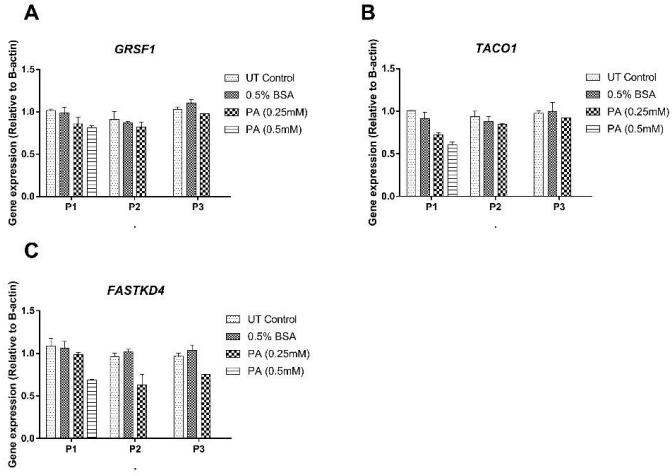

Figure 7: Gene expression profile of mtRNA binding proteins involved in mtRNA processing in HepG2 cells treated with 0.25mmol/l palmitic acid (PA) for 1 or 2 weeks (**P1, P2**) followed by an additional 2 weeks (**P3**) on resuscitation medium without any PA. A) *GRSF1*; B) *TACO1*; C) *FASTKD4*. (n=1).

Mice on a high fat diet show increased mtDNA methylation in the *Nd6* gene

Since no clear induction of mtDNA methylation was observed in PA-exposed HepG2 cells, we assessed whether the increased methylation of *ND6* observed in NASH patients by others[7] could be explained by the *in vivo* context of inflammation and fibrosis. In order to study this, mice were fed with a high fat-high cholesterol diet (HFC) for 20 weeks to mimic advanced stages resembling NASH (lipid accumulation associated with inflammation and fibrosis; 20wkHFC), as described earlier[43,44]. Induction of fibrosis in the 20wkHFC model was confirmed by increased hepatic expression of fibrotic markers, *Col1a1* and *Acta2* (data not shown). MtDNA was

pyrosequenced for the D-loop, *Cox1,* and *Nd6* regions for these 20wkHFC-fed mice and normal chow-fed mice. Interestingly, in line with the previous findings in humans, significant increases in methylation were observed in the *Nd6* gene in mice at positions 13,857 ($p<0.001$) and 13,926 ($p<0.05$) (**Figure 8A**) compared to the control-fed mice. No differential methylation was observed in the *Cox1* gene for 20wkCD compared to the 20wkHFC groups (**Figure 8B**). However, methylation within the D-loop region was lower at the two CpG positions 15,826 and 15,866 ($p<0.05$) for 20wkHFC-fed mice compared to the control-fed animals (**Figure 8C).**

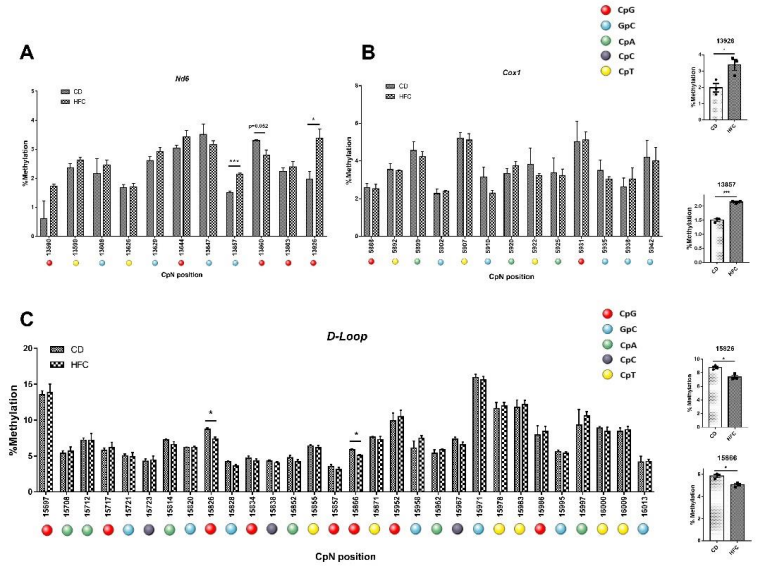

Figure 8: Pyrosequencing on whole mouse liver. MtDNA from mice on high fat and cholesterol diet (HFC) versus chow diet (CD) for 20 weeks was assessed for methylation. The analyzed regions include; A) *ND6*; B) *COX1* and; C) mtDNA *D-loop*. Data represent the mean ± SEM. *p≤0.05, **p<0.01 and ***p<0.001 with respect to the chow control (n=3).

Interestingly, *Nd6* expression was significantly increased ($p<0.05$) in these mice as well as in mice mimicking early stages of NAFLD (lipid accumulation and mild inflammation, without fibrosis; 6wkHFC) when compared to control-fed animals (**Figure 9A,B,E**). Inflammation and fibrosis markers were not increased in 6wkHFC mice compared to control-fed animals (data not shown), confirming that the disease state indeed had not yet progressed to NASH. *CytB* expression also showed a trend towards increased expression ($p = 0.065$) in 6wkHFC mice, with no change in *Cox1*

expression (**Figure 9C, D**). In the 20wkHFC mice, no changes in mitochondrial content and gene expression for *CytB* and *Cox1* were observed in comparison to the control-fed animals (**Figure 9F-H**).

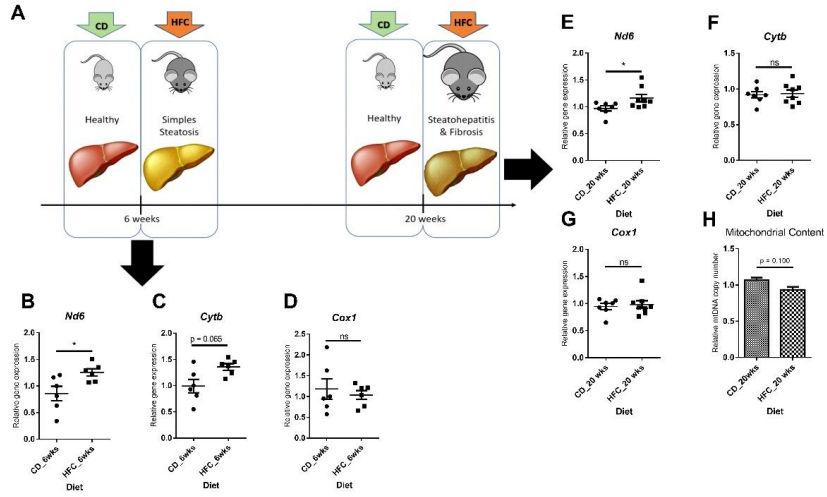

Figure 9: Gene expression of three mitochondrial genes and mitochondrial content in mice on high fat and cholesterol diet (HFC) versus chow diet (CD) for 6 weeks and 20 weeks. A) Schematic diagram showing experimental set-up. Mitochondrial gene expression in CD versus HFC after 6 weeks: B) *Nd6*; C) *CytB*; D) *Cox1*. Mitochondrial gene expression in CD versus HFC after 6 weeks: E) *Nd6*; F) *CytB*; G) *Cox1*; H) Mitochondrial copy number. Data represent the mean ± SEM. *p≤0.05, **p<0.01 and ***p<0.001 with respect to the CD control animals.

Next, we determined whether the two mouse models could be compared to provide insight in NAFLD progression. Importantly, expression levels of mitochondrial genes were similar in both 6-week and 20-week control-fed groups (**Supplementary Figure S7A-C**). The increase in expression of *Nd6* was similar for the 6wkHFC versus the 20wkHFC mice (**Supplementary Figure S7D**), and the unresponsiveness in expression of *Cox1* was seen for both models (**Supplementary Figure S7E**). Interestingly, the trend towards an initial increase in *CytB* expression at 6wkHFC (1.4 ± 0.2 compared to control diet, **Figure 9C**) (p=0.065) returned to control levels in 20wkHFC mice (0.9 ± 0.1) (**Supplementary Figure S7F**).

Human Liver

Next, we analyzed steatotic liver samples from morbid obese individuals who had underwent bariatric surgery and compared to non-steatotic human liver tissue. While hepatic mRNA levels of *PNPLA3*, a biomarker of NAFLD, were significantly enhanced in liver tissue obtained during bariatric surgery when compared to non-steatotic human liver, expression of inflammatory (*TNFα, IL1β*) and fibrotic markers (*COL1A1, ACTA2*) in these patients was not increased (data not shown). Interestingly, similar to the mice, *ND6* expression was significantly higher in steatotic livers ($p<0.01$) compared to the healthy controls (**Figure 10A, B**). Other mitochondrial genes, such as *CYTB, COX1*, *12S* and *16S,* were also significantly elevated ($p<0.05$) compared to the healthy controls (**Figure 10C-E**). Intriguingly, the overall increase in gene expression was not associated with an increase in mtDNA copy number between steatotic and non-steatotic human livers (**Figure 10F**).

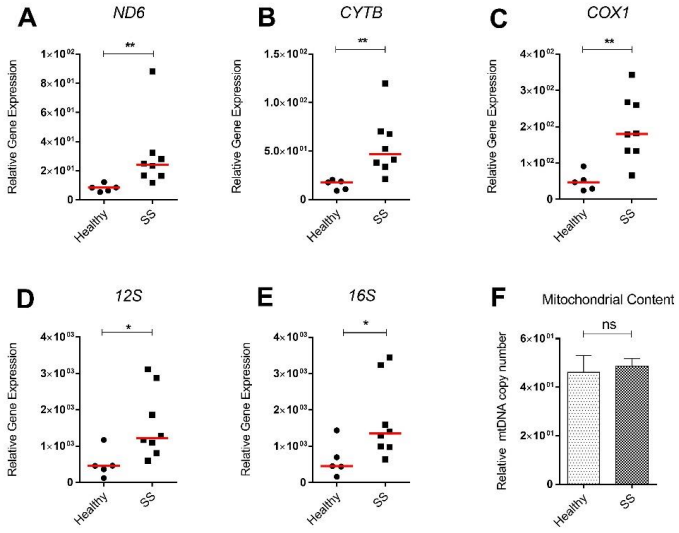

Figure 10: Relative mitochondrial gene expression and mtDNA copy number in whole human liver samples from obese bariatric surgery patients (with SS). Human liver samples from bariatric surgery patients were obtained. These liver samples had characteristics of SS. mRNA expression of A) *ND6*; B) *COX1*; C) *CYTB*; D) *12S*; E) *16S* genes and F) mitochondrial copy number. All relative to *β-actin* mRNA or DNA. Red line represents the median. *p≤0.05, **p<0.01 and ***p<0.001 with respect to the control.

Using the previously described primers for methylation-specific PCR[7], we confirmed the increase in *ND6* methylation in steatotic livers compared to non-steatotic livers (methylated/unmethylated DNA ratio of 0.62 and 0.50, respectively; p<0.05) (**Figure 11A**). No changes in methylation were found for the D-loop and the *COX1* gene (**Figure 11B, C**). Surprisingly, for *ND6*, no increases in methylation were observed using pyrosequencing (**Figure 11D**), reflecting a low contribution of position 14476 as one of the three cytosines being interrogated by MSP.

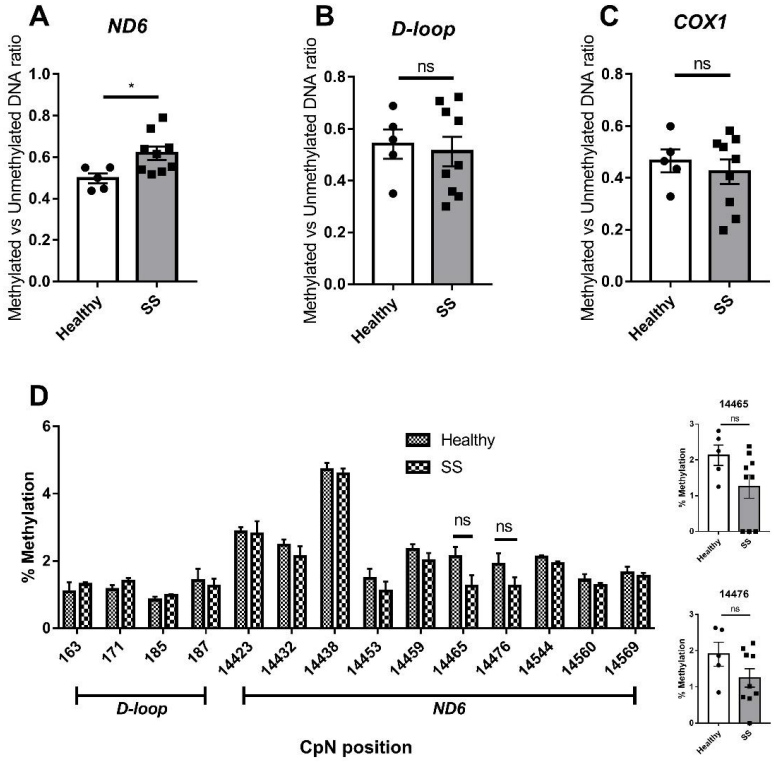

Figure 11: Methylation specific PCR (MSP) and pyrosequencing on whole human liver samples from obese bariatric surgery patients (with SS). Methylation Specific PCR on **A)** *ND6*; **B)** *D-loop*; **C)** *COX1* on healthy controls (n=5) versus SS patients (n=9); **D)** *D-loop* [163-187] and *ND6* [14423 – 14569] pyrosequencing on healthy controls versus SS patients. Significance is demonstrated as *p≤0.05, **p<0.01 and ***p<0.001 with respect to the healthy controls.

In addition, analysis of a publicly available RNAseq database[47] (**Supplementary Figure S8**) also points to differential mitochondrial gene expression between patients with different stages of NAFLD and healthy normal-weight individuals. Interestingly, in

line with our observation, *ND6* gene expression was significantly increased in patients with NAFLD compared to healthy normal-weight individuals. *ND5* and *CYTB* also showed an increase in expression while *RNR1, COX3,* and *ND4L* showed a decrease in expression in patients with NAFLD compared to healthy normal-weight individuals.

DISCUSSION

We here set out to unravel a role for mtDNA methylation in NAFLD, based on a report describing that *ND6* methylation was higher, associated with lower *ND6* expression, in liver samples of NASH patients compared to SS patients[7]. Our studies in NAFLD mouse models and patient samples confirmed an increase in mtDNA methylation in the *ND6* gene in NAFLD. In contrast, we found the *ND6* expression to be higher for our *in vivo* NAFLD samples compared to healthy samples. To provide mechanistic insights, we exposed liver cells to fatty acids and created transgenic liver cell lines. We demonstrate that i) mtDNA methylation decreased overall mitochondrial gene expression, which ii) caused mitochondrial dysfunction and iii) promoted lipid accumulation, while iv) lipid exposure did not induce mtDNA methylation.

The lack of effect on mtDNA methylation in our 2 week PA exposure studies excludes an immediate causal role for PA on mtDNA methylation, although other dietary lipids have been shown to induce hepatic mtDNA methylation in fish[51]. The PA treatment did modulate gene expression levels, including an upregulation of nuclear *PPARGC1A*. In another study, 48 hours PA exposure of muscle cells resulted in a downregulation of nuclear *PPARGC1A* expression which impaired mitochondrial biogenesis[52]. Also NASH patients show reduced expression of nuclear-encoded mitochondrial proteins (PGC1α, NRF1 and TFAM) and of mitochondrial proteins that constitute complex I, II, IV and V of the ETC[9]. Although we did not find reduced expression of the nuclear genes, mtDNA copy number and mtDNA gene expression generally was repressed by PA. Interestingly, despite the lower copy number, *ND6* expression was restored during the second week of PA treatment. This relative increase in expression of *ND6* compared to other mitochondrially encoded genes is in line with the increase only observed for *Nd6* expression in our mouse models. In addition, exploring a RNAseq database, *ND6* was the highest upregulated gene in human steatotic livers compared to healthy normal-weight individuals.

Also, in our SS patient samples, an increase in *ND6* expression was observed compared to healthy liver samples. This finding on increased *ND6* expression seems in contrast to the earlier human study[7], which reported a decreased *ND6* expression in NASH compared to simple steatosis. In this respect, it is important to note that we

normalized the expression data against *β-actin*, and not against *12S* or *16S*[7], which we here and previously[19] found to be regulated by mtDNA methylation. Yet, the initial *ND6* increase as reported by us for SS, followed by a decrease when progressing to NASH[7], would fit a proposed compensation model of dynamic regulation of mtDNA copy number as a response to mitochondrial dysfunction during disease severity[53-55]. Indeed, an increase in mtDNA copy number has been reported in patients with simple steatosis compared to healthy controls while a reduction in mtDNA copies was observed in NASH patients compared to patients with simple steatosis[10,56]. Also, an increase in mtDNA copy number has been reported in mitochondrial diseases like myopathy and amyotrophic lateral sclerosis (ALS)[57,58]. Although we did not detect an increase in copy number in livers of our SS samples or 20wkHFC-mice, the trend towards higher mtDNA copy number upon artificial induction of CpG/GpC methylation in HepG2 cells might indeed reflect an initial compensation mechanism to counter the decrease in mitochondrial function.

Mitochondrial DNA methylation would add an additional layer to such dynamic regulation processes. Although we could confirm the higher *ND6* methylation in NAFLD in mice using pyrosequencing and in human using the previously reported CpG-focused MSP approach[7], we could not pin point particular essential cytosines using pyrosequencing in the human SS samples. Yet, the indirect influence of DNA methylation (e.g. through inhibition of DNMT1) on *ND6* expression has been indicated by others[7,34,59]. As *ND6* expression is under the control of the LSP promoter, the inverse relationship between LSP promoter methylation and *ND6* expression as indicated by our transgenic HepG2 cells and confirmed by others[33], should be explored in more detail on NAFLD samples. The realization that mtDNA (supercoiled, protein-fixed structure with massive CnonG methylation, resulting in strand-specific patterns) requires somewhat different considerations compared to nuclear DNA$^{(merged)}$ but will eventually add to understanding this additional layer of regulation.

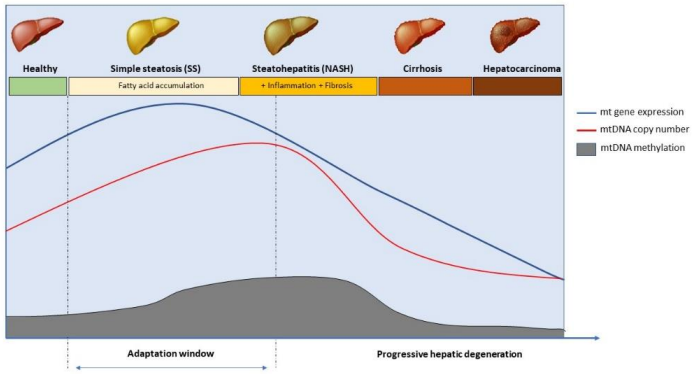

Figure 12: Schematic diagram showing the changes in mitochondrial gene expression, mtDNA methylation and mtDNA copy number during NAFLD progression. NAFLD is a progressive disease characterized by simple steatosis (SS), steatohepatitis (NASH) and it can later deteriorate to cirrhosis and hepatocarcinoma. During the initial simple steatotic phase, the liver's adaptation mechanisms are activated, and this is seen by an increase in mtDNA copy number and mitochondrial gene expression. However, as the disease progresses to NASH, mtDNA methylation increases and mitochondrial gene expression is impaired. During NASH, mtDNA hypermethylation reverses the positive correlation between mtDNA copy number and mitochondrial gene expression resulting in a loss of metabolic adaptation. The liver becomes more susceptible to lipid accumulation and monosaturated fatty acid induced downregulation of mtRNA processing proteins. Overall, this perpetuates mitochondrial dysfunction. Based on previous studies in cancer, as NAFLD progresses further to hepatocarcinoma, mtDNA copy number decreases and mtDNA becomes hypomethylated.

In conclusion, we show that artificially-methylated mtDNA promotes mitochondrial dysfunction and disturbs cellular lipid metabolism. Mitochondrial dysfunction presented as impaired activity of the ETC complexes is a hallmark of NAFLD[64]. In addition, epigenetic dysregulation has been reported in NAFLD, which is associated with aberrant nuclear gene expression and detrimental shifts in cellular metabolism[61-63]. Our finding supports a role for mtDNA methylation in NAFLD, and confirms another study[7]. The suggestion that differential mitochondrial DNA methylation affects mitochondrial functioning in NAFLD sheds an additional light on the underlying mechanisms (**Figure 12**). Yet, more regions and more samples in different stages of disease need to be included to better understand the dynamic nature of mtDNA responses. As epigenetic changes are reversible, as shown for *ND6* by physical exercise[7], and can be targeted by epigenetic-editing strategies[65,66], a better understanding of mtDNA methylation might also allow for innovative treatment options.

Indeed, targeted approaches are currently explored to remove mutated mitochondrial DNA from diseased cells. To remove DNA methylation, TET enzymes can be used which are already reaching mainstream applications for nuclear DNA[67,68]. Since TET enzymes also localize to mitochondria[69], with corresponding hydroxymethylation profiles, these approaches might turn out effective in treating mitochondrial dysfunction in a range of diseases.

ACKNOWLEDGEMENTS

Funding for this project was provided by the UMCG. A. Mposhi was funded through a talent development program at the UMCG. The authors would like to thank Dr. Ali Saeed from the University Medical Centre Groningen (UMCG) and Dr. Danial Afsharzadeh (UMCG) for their assistance with the patient and mouse liver material.

REFERENCES

1. Peng KY, Watt MJ, Rensen S, et al. Mitochondrial dysfunction-related lipid changes occur in nonalcoholic fatty liver disease progression. *J Lipid Res*. 2018;59(10):1977-1986.

2. McInnes J. Mitochondrial-associated metabolic disorders: Foundations, pathologies and recent progress. *Nutr Metab (Lond)*. 2013;10(1):63-7075-10-63.

3. Gray MW. Mitochondrial evolution. *Cold Spring Harb Perspect Biol*. 2012;4(9):a011403.

4. Campbell A, Mrazek J, Karlin S. Genome signature comparisons among prokaryote, plasmid, and mitochondrial DNA. *Proc Natl Acad Sci U S A*. 1999;96(16):9184-9189.

5. Anderson S, Bankier AT, Barrell BG, et al. Sequence and organization of the human mitochondrial genome. *Nature*. 1981;290(5806):457-465.

6. Rackham O, Shearwood AM, Mercer TR, Davies SM, Mattick JS, Filipovska A. Long noncoding RNAs are generated from the mitochondrial genome and regulated by nuclear-encoded proteins. *RNA*. 2011;17(12):2085-2093.

7. Pirola CJ, Gianotti TF, Burgueno AL, et al. Epigenetic modification of liver mitochondrial DNA is associated with histological severity of nonalcoholic fatty liver disease. *Gut*. 2013;62(9):1356-1363.

8. Mehta R, Jeiran K, Koenig AB, et al. The role of mitochondrial genomics in patients with non-alcoholic steatohepatitis (NASH). *BMC Med Genet*. 2016;17(1):63-016-0324-0.

9. Koliaki C, Szendroedi J, Kaul K, et al. Adaptation of hepatic mitochondrial function in humans with non-alcoholic fatty liver is lost in steatohepatitis. *Cell Metab*. 2015;21(5):739-746.

10. Kamfar S, Alavian SM, Houshmand M, et al. Liver mitochondrial DNA copy number and deletion levels may contribute to nonalcoholic fatty liver disease susceptibility. *Hepat Mon*. 2016;16(12):e40774.

11. Nicholls TJ, Minczuk M. In D-loop: 40 years of mitochondrial 7S DNA. *Exp Gerontol*. 2014;56:175-181.

12. Stewart JB, Chinnery PF. The dynamics of mitochondrial DNA heteroplasmy: Implications for human health and disease. *Nat Rev Genet*. 2015;16(9):530-542.

13. Holt IJ, Reyes A. Human mitochondrial DNA replication. *Cold Spring Harbor Perspectives in Biology*. 2012;4(12):a012971.

14. Litonin D, Sologub M, Shi Y, et al. Human mitochondrial transcription revisited: Only TFAM and TFB2M are required for transcription of the mitochondrial genes in vitro. *J Biol Chem*. 2010;285(24):18129-18133.

15. Blumberg A, Sri Sailaja B, Kundaje A, et al. Transcription factors bind negatively selected sites within human mtDNA genes. *Genome Biol Evol*. 2014;6(10):2634-2646.

16. Shokolenko IN, Alexeyev MF. Mitochondrial transcription in mammalian cells. *Frontiers in bioscience (Landmark edition)*. 2017;22:835-853.

17. Mposhi A, Van der Wijst MG, Faber KN, Rots MG. Regulation of mitochondrial gene expression, the epigenetic enigma. *Front Biosci (Landmark Ed)*. 2017;22:1099-1113.

18. van der Wijst MG, Rots MG. Mitochondrial epigenetics: An overlooked layer of regulation? *Trends Genet*. 2015; 31(7):353-6

19. van der Wijst MG, van Tilburg AY, Ruiters MH, Rots MG. Experimental mitochondria-targeted DNA methylation identifies GpC methylation, not CpG methylation, as potential regulator of mitochondrial gene expression. *Sci Rep*. 2017;7(1):177-017-00263-z. Epub 2017 Mar 14.

20. Dou X, Boyd-Kirkup JD, McDermott J, et al. The strand-biased mitochondrial DNA methylome and its regulation by DNMT3A. *Genome Res*. 2019;29(10):1622-1634.

21. Feng S, Xiong L, Ji Z, Cheng W, Yang H. Correlation between increased ND2 expression and demethylated displacement loop of mtDNA in colorectal cancer. *Mol Med Rep*. 2012;6(1):125-130.

22. Gao J, Wen S, Zhou H, Feng S. De-methylation of displacement loop of mitochondrial DNA is associated with increased mitochondrial copy number and nicotinamide adenine dinucleotide subunit 2 expression in colorectal cancer. *Mol Med Rep*. 2015;12(5):7033-7038.

23. Sun X, Vaghjiani V, Jayasekara WSN, Cain JE, St John JC. The degree of mitochondrial DNA methylation in tumor models of glioblastoma and osteosarcoma. *Clin Epigenetics*. 2018;10(1):157-018-0590-0.

24. Bartelli TF, Bruno DCF, Briones MRS. Evidence for mitochondrial genome methylation in the yeast candida albicans: A potential novel epigenetic mechanism affecting adaptation and pathogenicity? *Front Genet*. 2018;9:166.

25. Byun HM, Panni T, Motta V, et al. Effects of airborne pollutants on mitochondrial DNA methylation. *Part Fibre Toxicol*. 2013;10:18-8977-10-18.

26. Byun HM, Colicino E, Trevisi L, Fan T, Christiani DC, Baccarelli AA. Effects of air pollution and blood mitochondrial DNA methylation on markers of heart rate variability. *J Am Heart Assoc*. 2016;5(4):10.1161/JAHA.116.003218.

27. Breton CV, Song AY, Xiao J, et al. Effects of air pollution on mitochondrial function, mitochondrial DNA methylation, and mitochondrial peptide expression. *Mitochondrion*. 2019;46:22-29.

28. Vos S, Nawrot TS, Martens DS, Byun HM, Janssen BG. Mitochondrial DNA methylation in placental tissue: A proof of concept study by means of prenatal environmental stressors. *Epigenetics*. 2020:1-11.

29. Sanyal T, Bhattacharjee P, Bhattacharjee S, Bhattacharjee P. Hypomethylation of mitochondrial D-loop and ND6 with increased mitochondrial DNA copy number in the arsenic-exposed population. *Toxicology*. 2018;408:54-61.

30. Zheng LD, Linarelli LE, Liu L, et al. Insulin resistance is associated with epigenetic and genetic regulation of mitochondrial DNA in obese humans. *Clin Epigenetics*. 2015;7(1):60-015-0093-1. eCollection 2015.

31. Blanch M, Mosquera JL, Ansoleaga B, Ferrer I, Barrachina M. Altered mitochondrial DNA methylation pattern in alzheimer disease-related pathology and in parkinson disease. *Am J Pathol*. 2016;186(2):385-397.

32. Bellizzi D, D'Aquila P, Scafone T, et al. The control region of mitochondrial DNA shows an unusual CpG and non-CpG methylation pattern. *DNA Res*. 2013;20(6):537-547.

33. Patil V, Cuenin C, Chung F, et al. Human mitochondrial DNA is extensively methylated in a non-CpG context. *Nucleic Acids Res*. 2019.

34. Shock LS, Thakkar PV, Peterson EJ, Moran RG, Taylor SM. DNA methyltransferase 1, cytosine methylation, and cytosine hydroxymethylation in mammalian mitochondria. *Proc Natl Acad Sci U S A*. 2011;108(9):3630-3635.

35. Saini SK, Mangalhara KC, Prakasam G, Bamezai RNK. DNA Methyltransferase1 (DNMT1) Isoform3 methylates mitochondrial genome and modulates its biology. *Sci Rep*. 2017;7(1):1525-017-01743-y.

36. Wong M, Gertz B, Chestnut BA, Martin LJ. Mitochondrial DNMT3A and DNA methylation in skeletal muscle and CNS of transgenic mouse models of ALS. *Front Cell Neurosci*. 2013;7:279.

37. Liu B, Du Q, Chen L, et al. CpG methylation patterns of human mitochondrial DNA. *Sci Rep*. 2016;6:23421.

38. Owa C, Poulin M, Yan L, Shioda T. Technical adequacy of bisulfite sequencing and pyrosequencing for detection of mitochondrial DNA methylation: Sources and avoidance of false-positive detection. *PLoS One*. 2018;13(2):e0192722.

39. Mechta M, Ingerslev LR, Fabre O, Picard M, Barres R. Evidence suggesting absence of mitochondrial DNA methylation. *Front Genet*. 2017;8:166.

40. Hong EE, Okitsu CY, Smith AD, Hsieh CL. Regionally specific and genome-wide analyses conclusively demonstrate the absence of CpG methylation in human mitochondrial DNA. *Mol Cell Biol*. 2013;33(14):2683-2690.

41. Bellizzi D, D'Aquila P, Scafone T, et al. The control region of mitochondrial DNA shows an unusual CpG and non-CpG methylation pattern. *DNA Res*. 2013;20(6):537-547.

42. Infantino V, Castegna A, Iacobazzi F, et al. Impairment of methyl cycle affects mitochondrial methyl availability and glutathione level in down's syndrome. *Mol Genet Metab*. 2011;102(3):378-382.

43. Sydor S, Gu Y, Schlattjan M, et al. Steatosis does not impair liver regeneration after partial hepatectomy. *Lab Invest*. 2013;93(1):20-30.

44. Bartuzi P, Billadeau DD, Favier R, et al. CCC- and WASH-mediated endosomal sorting of LDLR is required for normal clearance of circulating LDL. *Nat Commun*. 2016;7:10961.

45. Livak KJ, Schmittgen TD. Analysis of relative gene expression data using real-time quantitative PCR and the 2(-delta delta C(T)) method. *Methods*. 2001;25(4):402-408.

46. Gomes AP, Price NL, Ling AJ, et al. Declining NAD(+) induces a pseudohypoxic state disrupting nuclear-mitochondrial communication during aging. *Cell*. 2013;155(7):1624-1638.

47. Suppli MP, Rigbolt KTG, Veidal SS, et al. Hepatic transcriptome signatures in patients with varying degrees of nonalcoholic fatty liver disease compared with healthy normal-weight individuals. *Am J Physiol Gastrointest Liver Physiol*. 2019;316(4):G462-G472.

48. Zeng Z, Meyer KF, Lkhagvadorj K, et al. Prenatal smoke effect on mouse offspring Igf1 promoter methylation from fetal stage to adulthood is organ and sex specific. *Am J Physiol Lung Cell Mol Physiol*. 2020;318(3):L549-L561.

49. Alkhouri N, Dixon LJ, Feldstein AE. Lipotoxicity in nonalcoholic fatty liver disease: Not all lipids are created equal. *Expert Rev Gastroenterol Hepatol*. 2009;3(4):445-451.

50. Li ZZ, Berk M, McIntyre TM, Feldstein AE. Hepatic lipid partitioning and liver damage in nonalcoholic fatty liver disease: Role of stearoyl-CoA desaturase. *J Biol Chem*. 2009;284(9):5637-5644.

51. Liao K, Yan J, Mai K, Ai Q. Dietary olive and perilla oils affect liver mitochondrial DNA methylation in large yellow croakers. *J Nutr*. 2015;145(11):2479-2485.

52. Barres R, Osler ME, Yan J, et al. Non-CpG methylation of the PGC-1alpha promoter through DNMT3B controls mitochondrial density. *Cell Metab*. 2009;10(3):189-198.

53. Hosnijeh FS, Lan Q, Rothman N, et al. Mitochondrial DNA copy number and future risk of B-cell lymphoma in a nested case-control study in the prospective EPIC cohort. *Blood*. 2014;124(4):530-535.

54. Liu CS, Cheng WL, Lee CF, et al. Alteration in the copy number of mitochondrial DNA in leukocytes of patients with mitochondrial encephalomyopathies. *Acta Neurol Scand*. 2006;113(5):334-341.

55. Lee HC, Wei YH. Mitochondrial biogenesis and mitochondrial DNA maintenance of mammalian cells under oxidative stress. *Int J Biochem Cell Biol*. 2005;37(4):822-834.

56. Tapia MAP, Fragoso-Bargas N, Rodríguez-Ríos D, Lazo-de-la-Vega-Monroy ML, del Rocío Ibarra-Reynoso L, Ruíz-Noa Y, del Carmen Preciado-Puga M, Velazquez-Villafaña M, Jordan-Pérez B, Garnelo-Cabañes S, García-Ramírez JR, Lund G. Peripheral blood mitochondrial DNA copy number, a potential marker of non-alcoholic fatty liver disease? *FASEB*. 2018;32(1):925.

57. Wredenberg A, Wibom R, Wilhelmsson H, et al. Increased mitochondrial mass in mitochondrial myopathy mice. *Proc Natl Acad Sci U S A*. 2002;99(23):15066-15071.

58. Stoccoro A, Mosca L, Carnicelli V, et al. Mitochondrial DNA copy number and D-loop region methylation in carriers of amyotrophic lateral sclerosis gene mutations. *Epigenomics*. 2018;10(11):1431-1443.

59. Mishra M, Kowluru RA. Epigenetic modification of mitochondrial DNA in the development of diabetic retinopathy. *Invest Ophthalmol Vis Sci*. 2015;56(9):5133-5142.

60. Matsuda S, Yasukawa T, Sakaguchi Y, et al. Accurate estimation of 5-methylcytosine in mammalian mitochondrial DNA. *Sci Rep*. 2018;8(1):5801-018-24251-z.

61. Gerhard GS, Malenica I, Llaci L, et al. Differentially methylated loci in NAFLD cirrhosis are associated with key signaling pathways. *Clin Epigenetics*. 2018;10(1):93-018-0525-9.

62. de Mello VD, Matte A, Perfilyev A, et al. Human liver epigenetic alterations in non-alcoholic steatohepatitis are related to insulin action. *Epigenetics*. 2017;12(4):287-295.

63. Pirola CJ, Scian R, Gianotti TF, et al. Epigenetic modifications in the biology of nonalcoholic fatty liver disease: The role of DNA hydroxymethylation and TET proteins. *Medicine (Baltimore)*. 2015;94(36):e1480.

64. Perez-Carreras M, Del Hoyo P, Martin MA, et al. Defective hepatic mitochondrial respiratory chain in patients with nonalcoholic steatohepatitis. *Hepatology*. 2003;38(4):999-1007.

65. de Groote ML, Verschure PJ, Rots MG. Epigenetic editing: Targeted rewriting of epigenetic marks to modulate expression of selected target genes. *Nucleic Acids Res*. 2012;40(21):10596-10613.

66. Thakore PI, Black JB, Hilton IB, Gersbach CA. Editing the epigenome: Technologies for programmable transcription and epigenetic modulation. *Nat Methods*. 2016;13(2):127-137.

67. Xu X, Tan X, Tampe B, et al. High-fidelity CRISPR/Cas9- based gene-specific hydroxymethylation rescues gene expression and attenuates renal fibrosis. *Nat Commun*. 2018;9(1):3509-018-05766-5.

68. Liu XS, Wu H, Ji X, et al. Editing DNA methylation in the mammalian genome. *Cell*. 2016;167(1):233-247.e17.

69. Dzitoyeva S, Chen H, Manev H. Effect of aging on 5-hydroxymethylcytosine in brain mitochondria. *Neurobiol Aging*. 2012;33(12):2881-2891.

70. Bogenhagen DF, Martin DW, Koller A. Initial steps in RNA processing and ribosome assembly occur at mitochondrial DNA nucleoids. *Cell Metab*. 2014;19(4):618-629.

71. Lee C, Zeng J, Drew BG, et al. The mitochondrial-derived peptide MOTS-c promotes metabolic homeostasis and reduces obesity and insulin resistance. *Cell Metab*. 2015;21(3):443-454.

72. Liu X, Trakooljul N, Hadlich F, Murani E, Wimmers K, Ponsuksili S. Mitochondrial-nuclear crosstalk, haplotype and copy number variation distinct in muscle fiber type, mitochondrial respiratory and metabolic enzyme activities. *Sci Rep*. 2017;7(1):14024-017-14491-w.

73. Dostal V, Churchill MEA. Cytosine methylation of mitochondrial DNA at CpG sequences impacts transcription factor A DNA binding and transcription. *Biochim Biophys Acta Gene Regul Mech*. 2019.

74. Kukat C, Davies KM, Wurm CA, et al. Cross-strand binding of TFAM to a single mtDNA molecule forms the mitochondrial nucleoid. *Proc Natl Acad Sci U S A*. 2015;112(36):11288-11293.

75. Farge G, Mehmedovic M, Baclayon M, et al. In vitro-reconstituted nucleoids can block mitochondrial DNA replication and transcription. *Cell Rep*. 2014;8(1):66-74.

76. Cagnone G, Tsai TS, Srirattana K, et al. Segregation of naturally occurring mitochondrial DNA variants in a mini-pig model. *Genetics*. 2016;202(3):931-944.

Supplementary Data and Tables

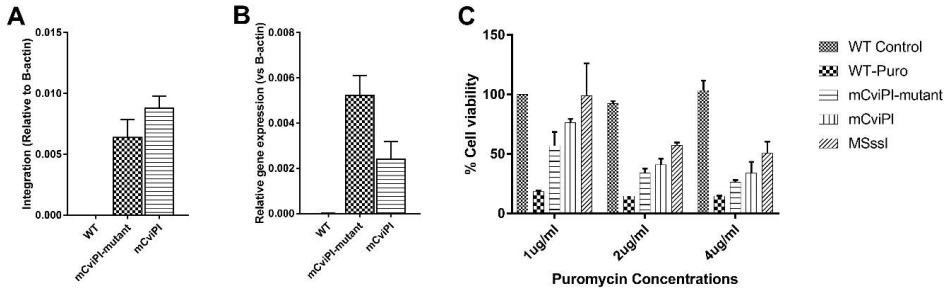

Supplementary Figure S1. **Validation of transgenic HepG2 cell lines. A-B**) Integration and gene expression of MCviPI in HepG2 cells; **C)** Puromycin selection of stable HepG2 cell line expressing MCviPI, MCviPI† (mutant) and MSssI versus WT Control (no puromycin) and WT-puro control (puromycin added).

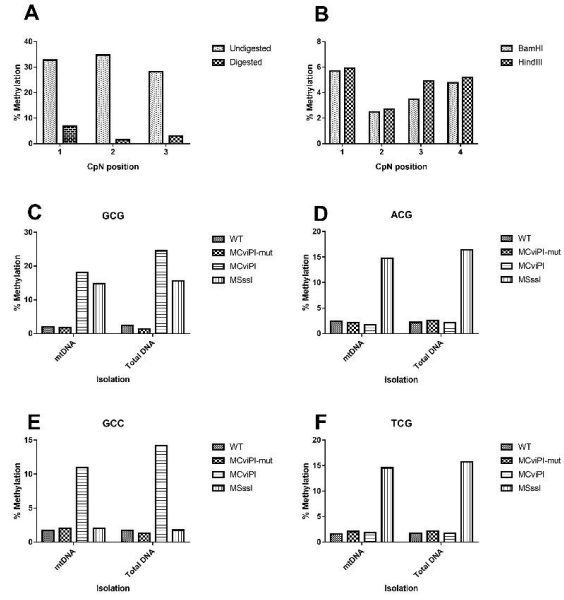

Supplementary Figure S2. MtDNA linearization and pyrosequencing of total genomic DNA versus mtDNA. A) Undigested versus *Bam*HI digested DNA; B) *Bam*HI versus *Hind*III digestion; C-F) Total genomic DNA versus mitochondrial DNA at CpG/GpC positions in HepG2 (wild type) and transgenic HepG2 lines expressing mitochondria targeted methyltransferases (mCviPI or MSssI).

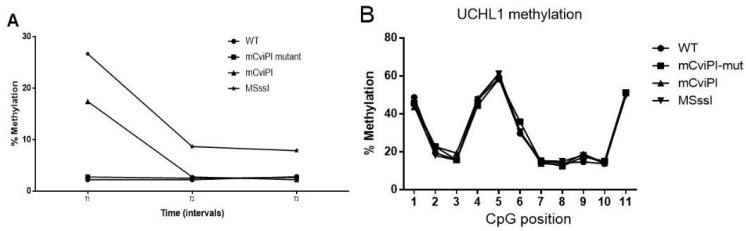

Supplementary Figure S3: Pyrosequencing. A) mtDNA methylation in HepG2 cells expressing MSssI and MCviPI over a 3-month period (T1 – T3) and; **B)** *UCHL1* promoter region methylation.

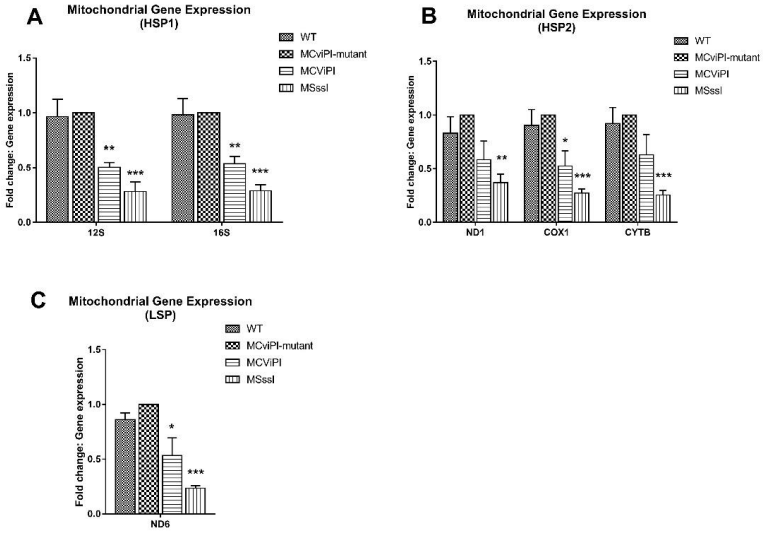

Supplementary Figure S4. Mitochondrial gene expression normalized to mtDNA copy number in transgenic HepG2 lines expressing mitochondria targeted methyltransferases (mCviPI or MSssI). Expression of A) *HSP1*; B) *HSP2* and; C) *LSP* genes normalized against HepG2-mtMCviPI mutant control and mtDNA copy number. Each data point represents the mean ± SEM of three independently constructed clones per transgenic cell line. Significance is demonstrated as *p≤0.05, **p<0.01 and ***p<0.001 with respect to the MCviPI mutant control.

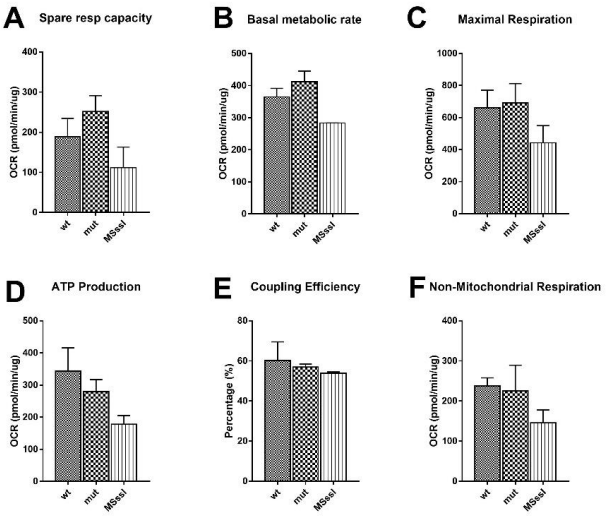

Supplementary Figure S5. Mitochondrial Oxygen consumption rate in HepG2 cells expressing mitochondria targeted methyltransferases (MSssI). A-F) Mitochondrial respiration was determined in HepG2- WT, HepG2-mCviPI-mutant and HepG2-MSssI. Each data point represents the mean ± SEM of two independently constructed transgenic cell.

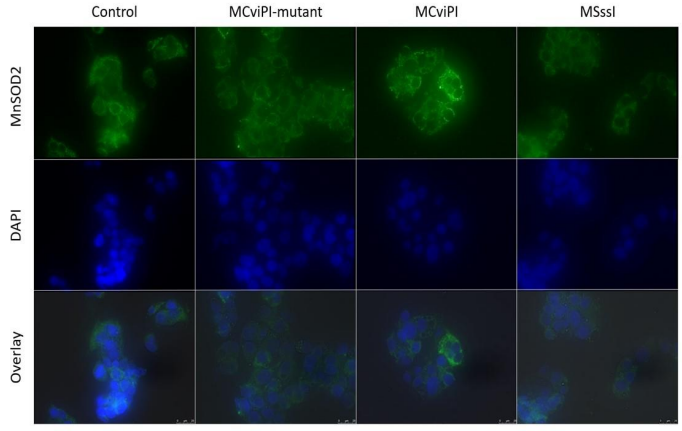

Supplementary Figure S6. Mitochondrial distribution and structure in HepG2 cells expressing mitochondria targeted methyltransferases. Fluorescence microscopy of wild type HepG2 and transgenic HepG2 cells expressing MCviPI†, MCviPI or MSssI. In order to stain mitochondria, cells were fixed with 4% parafolmaldehyde followed by blocking with 1% BSA. Cells were then incubated with anti-MnSOD2 (mitochondrial staining) at 4^{o}C overnight followed by incubation with the secondary antibody, Alexa488.

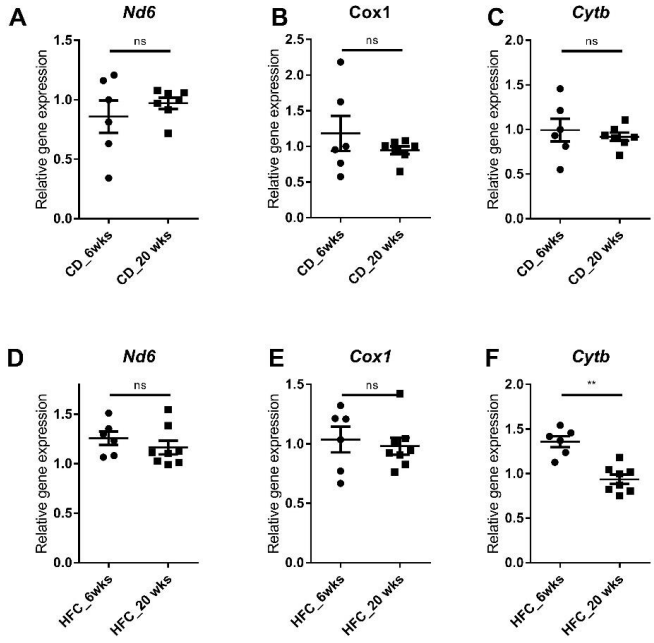

Supplementary Figure S7: Comparison of gene expression of three mitochondrial genes in mice on chow diet (CD) for 6 weeks versus 20 weeks: A) *Nd6*; B) *Cox1;* C) *CytB* and in mice on high fat and cholesterol diet (HFC) for 6 weeks versus 20 weeks: D) *Nd6*; E) *Cox1;* F) *CytB*. Data represent the mean ± SEM. *p≤0.05, **p<0.01 and ***p<0.001 with respect to the CD control animals

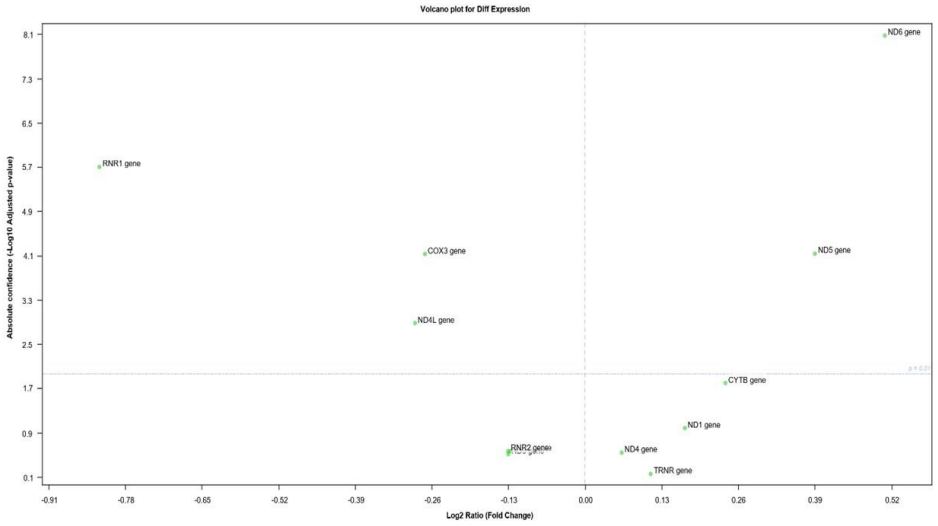

Supplementary Figure S8: Volcano plot showing differentially expressed mitochondrially encoded genes. Overview of differentially expressed mitochondrially encoded hepatic gene profiles between healthy normal-weight controls and non-alcoholic fatty liver disease (NAFLD) patients. Publicly available transcriptome dataset available on different stages of NAFLD downloaded from NCBI's Short Read Archive (SRA) database (http://www.ncbi.nlm.nih.gov/sra) under the accession number SRP186450. Sequenced reads were mapped to Homo sapiens mitochondrion, complete genome. 16569 bp, circular DNA (Accession #: NC_012920, version: NC_012920.1). The vertical axis (y-axis) corresponds to the mean expression value (absolute confidence) of log10 (q-value), and the horizontal axis (x-axis) displays the log2 fold change value. Positive x-values represent up-regulation and negative x-values represent down-regulation.

TABLES

Supplementary Table S1. Lentiviral transfection plasmid DNA ratios

Plasmid	Quantity (µg)
Vector	3
Gag/pol/rev	2
Envelope	1

Supplementary Table S2. Primers for mitochondrial DNA gene expression and copy number

Target	Forward primer 5′→3′	Reverse primer 5′→3′
ND1	ATACCCCCGATTCCGCTACGAC	GTTTGAGGGGGAATGCTGGAG
ND6	GGGTGGTGGTTGTGGTAAAC	CCCCGAGCAATCTCAATTAC
COX1	CGATGCATACACCACATGAA	AGCGAAGGCTTCTCAAATCA
CYTB	AATTCTCCGATCCGTCCCTA	GGAGGATGGGGATTATTGCT
12S	CTGCTCGCCAGAACACTACG	TGAGCAAGAGGTGGTGAGGT
16S	GTATGAATGGCTCCACGAGG	GGTCTTCTCGTCTTGCTGTG
PGC1a	TGAGAGGGCCAAGCAAAG	ATAAATCACACGGCGCTCTT
NRF1	GGGAGCTACAGTCACTATGG	TCCAGTAAGTGCTCCGAC
TFAM	CCGAGGTGGTTTTCATCTGT	TCCGCCCTATAAGCATCTTG
β-actin	CCAACCGCGAGAAGATGA	CCAGAGGCGTACAGGGATA
ND6 (M)	GTTGGAGTTATGTTGGAAGGAG	CAAAGATCACCCAGCTACTACC
COX1 (M)	CCCAGATATAGCATTCCCACG	ACTGTTCATCCTGTTCCTGC
CYTB (M)	CCCACCCCATATTAAACCCG	GAGGTATGAAGGAAAGGTATAAGGG
36B4 (M)	GCTTCATTGTGGGAGCAGACA	CATGGTGTTCTTGCCCATCAG
COX2 (M-dna)	ATAACCGAGTCGTTCTGCCAAT	TTTCAGAGCATTGGCCATAGAA
RSP18 (M-dna)	TGTGTTAGGGGACTGGTGGACA	CATCACCCACTTACCCCCAAAA

Supplementary Table S3. Pyrosequencing primers and design template

Region	LS/HS	Target Location	Sequences 5′→3′
D-loop (H)	LS	16412 - 16457	**Fw:** GGGTTATTTAGGTTTTATGATTTTGAAG **Rv:** ATAACACATTACAATCAAATCCCTTCTC **Seq:** GTTTATTTTAGTTATTTTTAAGTGT
D-loop (H)	LS	16084 - 16131	**Fw:** GGTTGATTGTTGTATTTGTTTGTAAGT **Rv:** CACCATTAACACCCAAAACTAAAATTCTA **Seq:** TTTATGTATTATAGGTGGTTAAG
D-loop (H)	HS	163 - 190	**Fw:** GTTTGGTGGAAATTTTTTGTTATGATGT **Rv:** CTTTAATTCCTACCTCATCCTATTATTT **Seq:** AATTAATATATTTTAGTAAGTATG
CYTB (H)	LS	15756 - 15812	**Fw:** TTAATTAGGGAGATAGTTGGTATTAGGA **Rv:** CAATAATCCCCATCCTCCATATATCC **Seq:** AGGATTGTTGTGAAGT
CSBII (H)	LS	275 - 316	**Fw:** GGAGGGGAAAATAATGTGTTAGT **Rv:** CCACTTTCCACACAAACATCATA **Seq:** TTTAAGTGTTGTGGTTAGA

CSBIII (H)	LS	329 - 366	**Fw:** GGAGTGGGAGGGGAAAAT **Rv:** CTCCCCCCCTTCTAACCACAAC **Seq:** TGGTTAGGTTGGTGT
HSP (H)	LS	526 - 583	**Fw:** AGTGTATTGTTTTGAGGAGGTAAG **Rv:** ACCCCCCAACTAACACATTATT **Seq:** GTTTTGAGGAGGTAAGTT
LSP (H)	LS	366 - 417	**Fw:** GAGTGGGAGGGGAAAATAATGTGTTA **Rv:** AACCACAACACTTAAACACATCTCTA **Seq:** GTTGGGGGGTGATTG
ND6 (H)	HS	14544 - 14569	**Fw:** GGGTTTGTGGGGTTTTTTTTTAAG **Rv:** TTAAACCCATATAACCTCCCCCAAAATTC **Seq:** TTTTATTTATGGGGGTTTAG
ND6 (H)	HS	14384 - 14476	**Fw:** GTGGTAGGGTGTGTTATTATTTTGAATT **Rv:** ACCACCCCATCATACTCT **Seq:** GATGGTTGTTTTTGGATA
COX1 (M)	HS	5888 - 5942	**Fw:** GTTGGAGTGTTATTTATTTTAGGTGTAAT **Rv:** AAAATTAAATCCCCTCCTCCA **Seq:** ATTAAATTTTATTATTTGTTTGAT
D-loop (M)	HS	15697 - 15723	**Fw:** TGTTATAAGGATATATTTGTGTTATTTGA **Rv:** ATTTCAATTTAACTACCCCCAAATTT **Seq:** TTATTTGGTTTATTAATTTATTATT
D-loop (M)	HS	15820 - 15871	**Fw:** GTTTATTAAATTTGGGGGTAGTTAAATTGA **Rv:** AAATACCAAATACATAACACCACAAT **Seq:** ATTTGGTTTTTATTTTAGGGTT
D-loop (M)	LS	15952 - 16013	**Fw:** GGAGAGTTAAAATTTGGTATTGAGTAGT **Rv:** ATCAACCCATAACCAACATAACTATAA **Seq:** GTTTTAGGTGATTGGG
ND6 (M)	LS	13590 - 13647	**Fw:** TTGGGAGATTGGTTGATGTATGA **Rv:** CTTTATATCATTCCTAATTAACATCATCTT **Seq:** GTTATGTTGGAAGGAGG
ND6 (M)	LS	13857 - 13926	**Fw:** GTGGGTTTGTTGGTTGTTTAATG **Rv:** CCCCAAATCTCTAAATATTCCTCAA **Seq:** TTAGGGTTTGGTGGA

D-loop: Displacement loop, **CYTB**: Cytochrome B, **CSBII/III**: Conserved sequence block 2/3, **HSP**: Heavy strand promoter, **LSP**: Light strand promoter, **ND6**: NADH-ubiquinone oxidoreductase subunit 6.

Supplementary Table S4. Methylation Specific PCR primers

		The primers sequences for methylation-specific PCR	
Gene	**Location**	**Forward primer 5′→3′**	**Reverse primer 5′→3′**
ND6-M	14242 - 14484	TTTCGTATTAATAGGATTTTTTCGA	AATTATCTTTAAATATACTACAACGAT
ND6-U	14242 - 14484	TTTTGTATTAATAGGATTTTTTTGA	ATAATTATCTTTAAATATACTACAACAAT
COX1-M	5948 - 6151	GGAATATTATATTTATTATTCGGCGT	ACTAATCAATTACCAAAACCTCCG
COX1-U	5948 - 6151	TGGAATATTATATTTATTATTTGGTGT	CTAATCAATTACCAAAACCTCCAAT
D-loop-M	38 - 144	TAGGAATTAAAGATAGATATTGCGA	ACTCTCCATACATTTAATATTTTCGTC
D-loop-U	38 - 144	GGTAGGAATTAAAGATAGATATTGTGA	ACTCTCCATACATTTAATATTTTCATC

*__M__, methylated-specific primers; __U__, unmethylated-specific primers